SLAC-PUB-12236
November 2006

Development of a Focusing DIRC*

J. Benitez, I. Bedajanek, + D.W.G.S. Leith, G. Mazaheri, B. Ratcliff,

K. Suzuki, J. Schwiening, J. Uher,+ and J. Va'vra*

Particle & Particle Astrophysics division, SLAC, Stanford, CA, USA

***Abstract* — Benefiting from the recent introduction of new fast vacuum-based photon detectors with a transit time spread of σ_{TTS}~30-150ps, we are developing a novel RICH detector capable of correcting the chromatic error through good time measurements; we believe that this is the first time such a technique has been demonstrated. We have built and successfully tested a particle identification detector called "Focusing DIRC." The concept of the prototype is based on the BaBar DIRC, with several important improvements: (a) much faster pixelated photon detectors based on Burle MCP-PMTs and Hamamatsu MaPMTs, (b) a focusing mirror which allows the photon detector to be smaller and less sensitive to background in future applications, (c) electronics allowing the measurement of single photon timing to better than σ ~100-200ps, which allows a correction of the chromatic error. The detector was tested in a SLAC 10GeV/c electron test beam. This detector concept could be used for particle identification at Super B-factory, ILC, GlueX, Panda, etc.**

Keywords: Photodetectors; Cherenkov detectors; RICH.

INTRODUCTION

The DIRC detector at the BaBar experiment provides excellent particle identification performance [1]. Based on this success, our group has been following an R&D program to develop an appropriate photon detector for future particle identification systems. One such idea, a focusing DIRC, would be capable not only of measuring an (x,y) coordinate for each photon with an angular resolution similar to the present BaBar DIRC, but, in addition, measuring each photon's time-of-propagation (TOP[1]) along the Fused Silica bar with ~150-200 ps single-photoelectron timing resolution or better (the present BaBar DIRC has a timing resolution of only σ ~1.6 ns). This precise timing allows a measurement of the Cherenkov angle, with a precision similar to that provided by the direct angular measurement. This will allow the suppression of the background by more than one order of magnitude and will potentially allow a possible correction of the chromatic error and thus improve the angle measurement substantially. The focusing element also removes the bar thickness as a term that contributes to resolution smearing. The small pixel size reduces the overall size of the photon detector compared to that used in BaBar, which also helps to reduce the background. Such a device could be important for a future Super B-factory, and could also be useful in an ILC detector, especially one like SiD without a gaseous tracking detector.

We have built the first prototype of a focusing DIRC and had two successful test beam runs with it. In these runs, we established that (a) the new photon detectors work as expected, based on our bench tests;

• Manuscript received on November 28, 2006.
Work supported by the Department of Energy, contract DEAC02-76SF00515.
+ Visiting from the Institute of Experimental and Applied Physics, Czech Technical University, CZ-12800 Prague 2, Czech Republic.
* Corresponding author: tel.: 650-926-2658; fax: 650-926-4178; e-mail: jjv@slac.stanford.edu.
1 Definition: $TOP(\Phi, \theta_c, \lambda) = [L/v_g(\lambda)]\, q_z(\Phi,\theta_c)$, θ_c - Cherenkov angle, L - distance of light travels in the bar, $v_g(\lambda)$ - group velocity of light, λ - photon wavelength, and $q_z(\Phi,\theta_c)$ - z-component of the unit velocity vector.

Presented at IEEE Nuclear Sciences Symposium, October 29, 2006, San Diego, CA.

(b) we can achieve similar Cherenkov angle resolution as the BaBar DIRC with much more compact and faster detectors; (c) we can achieve single-photon timing resolution at a level of 100-200 ps; (d) we can clearly observe the expected chromatic dispersion on a photon by photon basis; and finally, (e), we can correct the chromatic error through this timing measurement. In addition we have developed software analysis packages and a Geant 4 Monte Carlo simulation of the prototype.

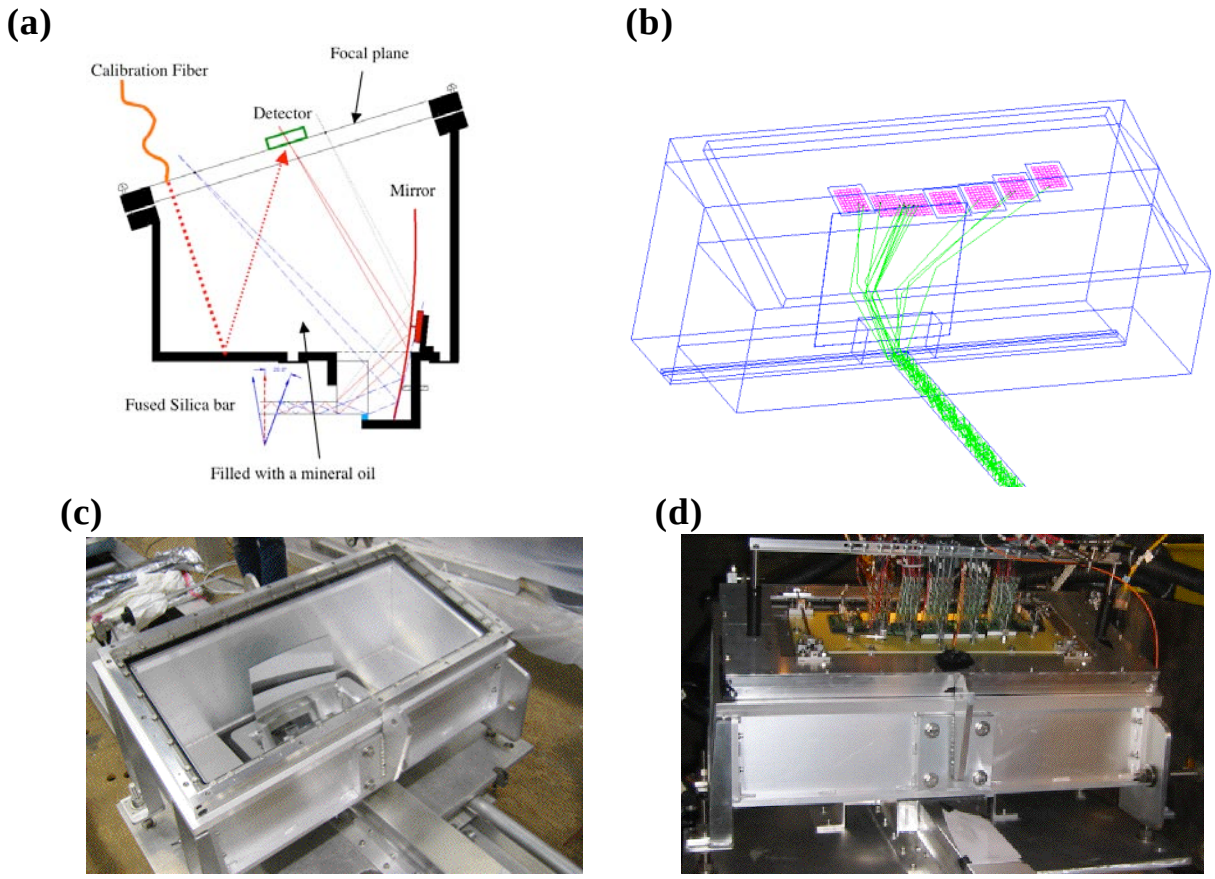

Fig. 1. (a) Principle of the Focusing DIRC prototype. (b) Geant 4 simulation of the photon propagation in the prototype. (c) Optical box, filled with mineral oil, shows a spherical mirror. (d) Electronics and photon detectors located on the focal plane, the optical box and the bar box with a bar entering the optical box.

PROTOTYPE DESCRIPTION

Figure 1 shows the concept and practical realization of the Fast Focusing DIRC prototype. This prototype is the first version of a "Focusing DIRC." The photon detectors used in this prototype will not work in a magnetic field.[2] The volume in the optical box between the Fused Silica bars and the photon detectors, is filled with a mineral oil. This prototype has a single DIRC bar of ~3.6 meters length, a focusing element made of a 50 cm focal length spherical mirror placed in a small optical box filled with mineral oil, which is the coupling medium between the bar and six 64-pixel photon detectors, and four Burle MCP-PMTs, and two Hamamatsu Flat-panel MaPMTs. The detailed studies of these photon detectors are described in detail in our two previous publications [2,3]. The system is instrumented with ~300 channels of electronics. We have developed fast amplifiers based on a pair of two Elantek 2075 chips producing a voltage gain of 130x with a ~1.5 ns rise time. The constant-fraction discriminators (CFD) are coupled to

[2] However, we have demonstrated that the Burle MCP-PMTs with smaller 10 micron hole diameter performs well at 15kG [4].

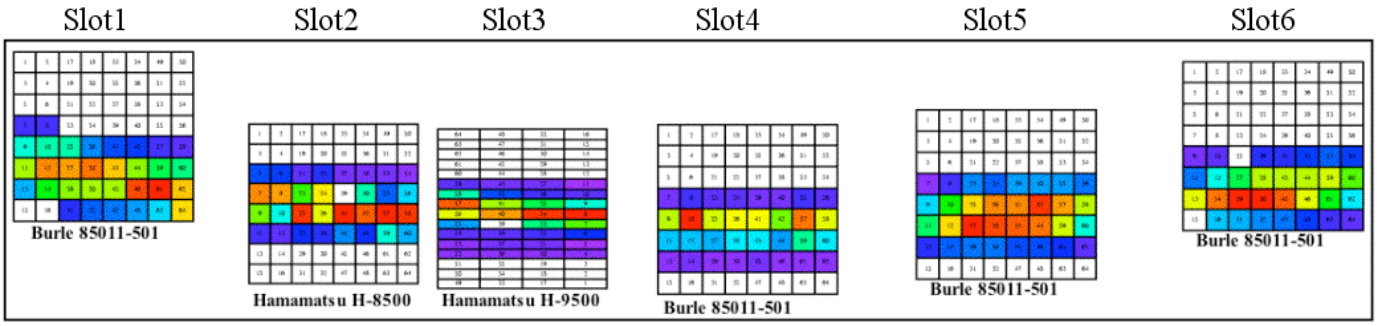

Fig. 2. Cherenkov ring measured in pixel domain. Slot 3 has the Hamamatsu MaPMT H-9500 where small pixels were interconnected into larger pads of 2.8x11.2mm^2 in size to provide finer sampling of the Cherenkov angle.

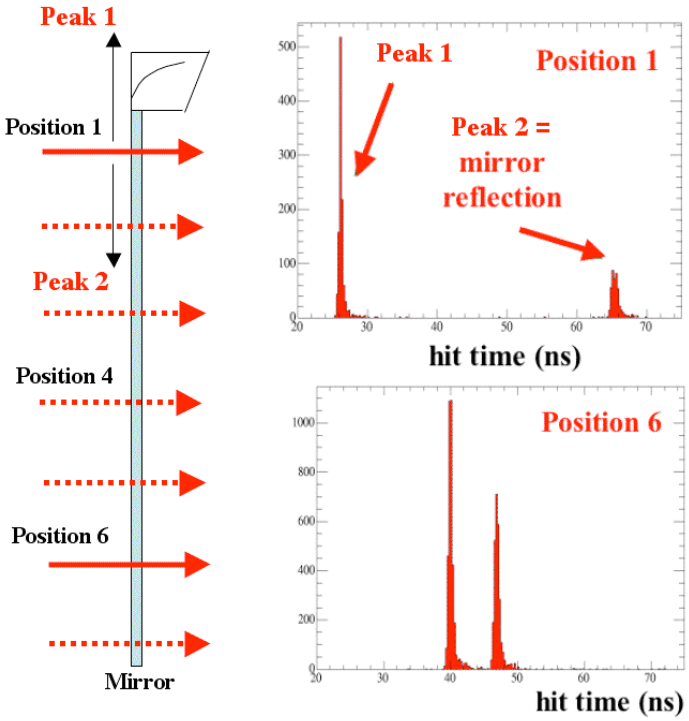

Fig. 3. Cherenkov ring measured in the time domain for different positions along the bar. The bar has a mirror at the far end to reflect indirect photons. The beam enters the bar perpendicularly.

Philips TDC7186, providing 25 ps/count. Fig. 1a shows how the prototype's spherical mirror is designed to remove the effect of bar thickness on the resolution. The photon detectors are located at the focal plane of the spherical mirror.[3] One should add that the prototype was designed to study the chromatic effects in the beam, and no effort was made to optimize it for any real application as a particle identification device. Fig. 1a also shows schematically a calibration system for the detectors using PiLas laser diode. The Cherenkov angle can be displayed either in the pixel domain (Fig.2), or in the time domain (Fig.3).

[3] Note that a real focal plane is not flat. A flat window is an approximation.

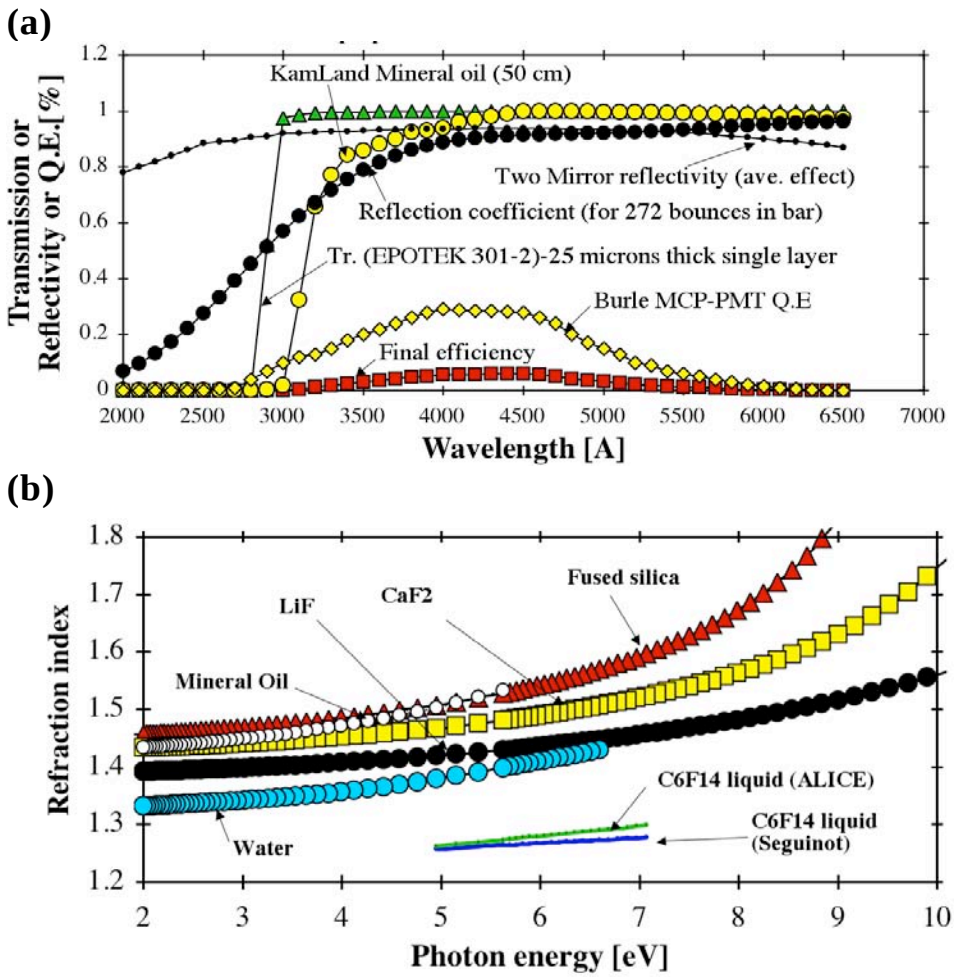

Fig. 4. (a) Various efficiencies in the Focusing DIRC prototype if placed into BaBar, assuming that we take Burle MCP-PMT quantum efficiency. (b) Refraction index of several materials, including water, mineral oil and Fused Silica.

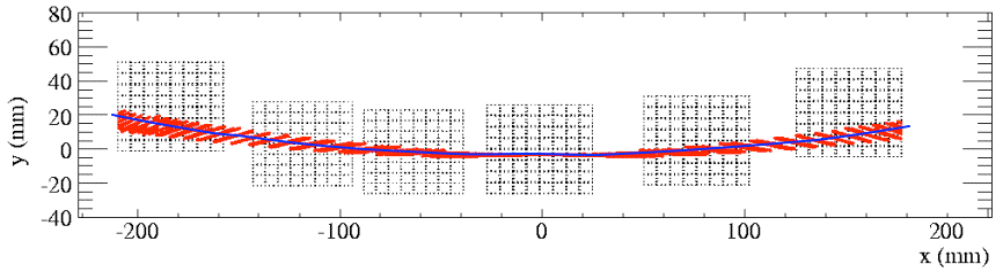

Fig. 5. The "spherical mirror/bar " aberration, generated by a simple ray-tracing program, creates rotated ring images at large values of abs(x), which worsens the average Cherenkov angle resolution. In blue we show expected ring without the aberration. The photons propagate over a few meters in the bar, and the detector response is assumed to be ideal in this simulation.

Figure 4a shows various efficiencies for a perpendicular track entering the Focusing DIRC prototype in the middle of its acceptance. In this design, the detector optical box is filled with mineral oil from the KamLand experiment, which simplifies the construction and makes it affordable at this particular stage. Its refraction index is a better match to Fused silica than water, as one can see in Fig. 4b. Table 1 compares contributions to the Cherenkov angle resolution of the present BaBar and what is expected for the Focusing DIRC prototype. Notice that the Focusing DIRC chromatic error is smaller than that of Babar DIRC. This

Table 1: Expected contributions to the Cherenkov angle resolution from various contributions:

Contribution to Cherenkov angle resolution [mrad]	**BaBar DIRC**	**Focusing DIRC Prototype** (# before correction, * after correction)
$\Delta\theta_{track}$	~1	~1
$\Delta\theta_{chromatic}$	~5.4	~3.5#, ~1*
$\Delta\theta_{"spherical\ mirror/bar"\ abberation}$	-	~4.5 (0 at ring center,~9 at ring wing)
$\Delta\theta_{transport\ along\ the\ bar}$	2-3	2-3
$\Delta\theta_{bar\ thickness}$	~4.1	-
$\Delta\theta_{PMT\ pixel\ size}$	~5.5	~5.5
$\Delta\theta_c^{track}$	~2.4	~1.5
Total $\Delta\theta_c^{photon}$	~9.6	~8.6#, 7.9*

Table 2: Burle MCP-PMT specifications:

Parameter	**H85011-501**
Photocathode type	Bialkali
Number of MCPs per PMT	2
Total average gain @ -2.3kV	~5x10^5
MCP hole diameter	25μm
MCP hole angle relative to perpendicular	12^o
Geometrical collection efficiency of the 1-st MCP	60-65%
Geometrical packing efficiency (for raw tube)	67%
Total fraction of "in time" photoelectrons detected[4]	**30-35%**
SLAC measurement of single electron resolution σ_{narrow} – pad center [ps]	50-70
Matrix of anode pixels	8 x 8
Pixel size [mm]	5.94 x 5.94
Pitch [mm]	6.45

Table 3: Hamamatsu H-8500 and H-9500 MaPMT specifications:

Parameter	**H-8500**	**H-9500**
Photocathode type	Bialkali	Bialkali
Number of dynodes	12	12
Total average gain @ -1kV	~10^6	~10^6
Geometrical collection efficiency of the 1-st dynode	70-80%	70-80%
Geometrical packing efficiency	97%	97%
Fraction of late photoelectron arrivals	~5%	~5%
Total fraction of "in time" photoelectrons detected[5]	**65-75%**	**65-75%**
SLAC measurement of single electron resolution σ_{narrow} – pad center [ps]	140	220
Matrix of anode pixels	8 x 8	16 x 16
Pixel size [mm]	5.8 x 5.8	2.8 x 2.8
Pitch [mm]	6.08	3.08

is believed to be due to two effects: (a) KamLand oil transparency cutoff above 300 nm [3], and (b) the Burle Bialkali quantum efficiency [3], which has higher red wavelength response (the average wavelength is 410nm). The Focusing DIRC has a new error contribution compared to the BaBar DIRC: its spherical mirror, together with a square bar, creates an aberration at larger ϕ angles (it is close to zero for ϕ ~0^o, and almost ~9 mrad at large ϕ) – see Fig. 5. We need to investigate how to reduce this error contribution in future

[4] Our measurements show that a typical relative efficiency of the Burle MCP-PMT is 50-60% of the 2 inch dia. Photonis XP 2262B PMT at 430nm, and drops to 30-50% around the edges [3]. In addition, the Burle MCP-PMT uniformity is ~1:1.5 [3].

[5] Using the same technique, we find that a relative efficiency of the Hamamatsu H-8500 MaPMT is 50-70% of the Photonis XP 2262B PMT at 430nm, and drops to 30-50% around the edges [3]. We also find that the Hamamatsu MaPMT uniformity is typically ~1:2.5 [3].

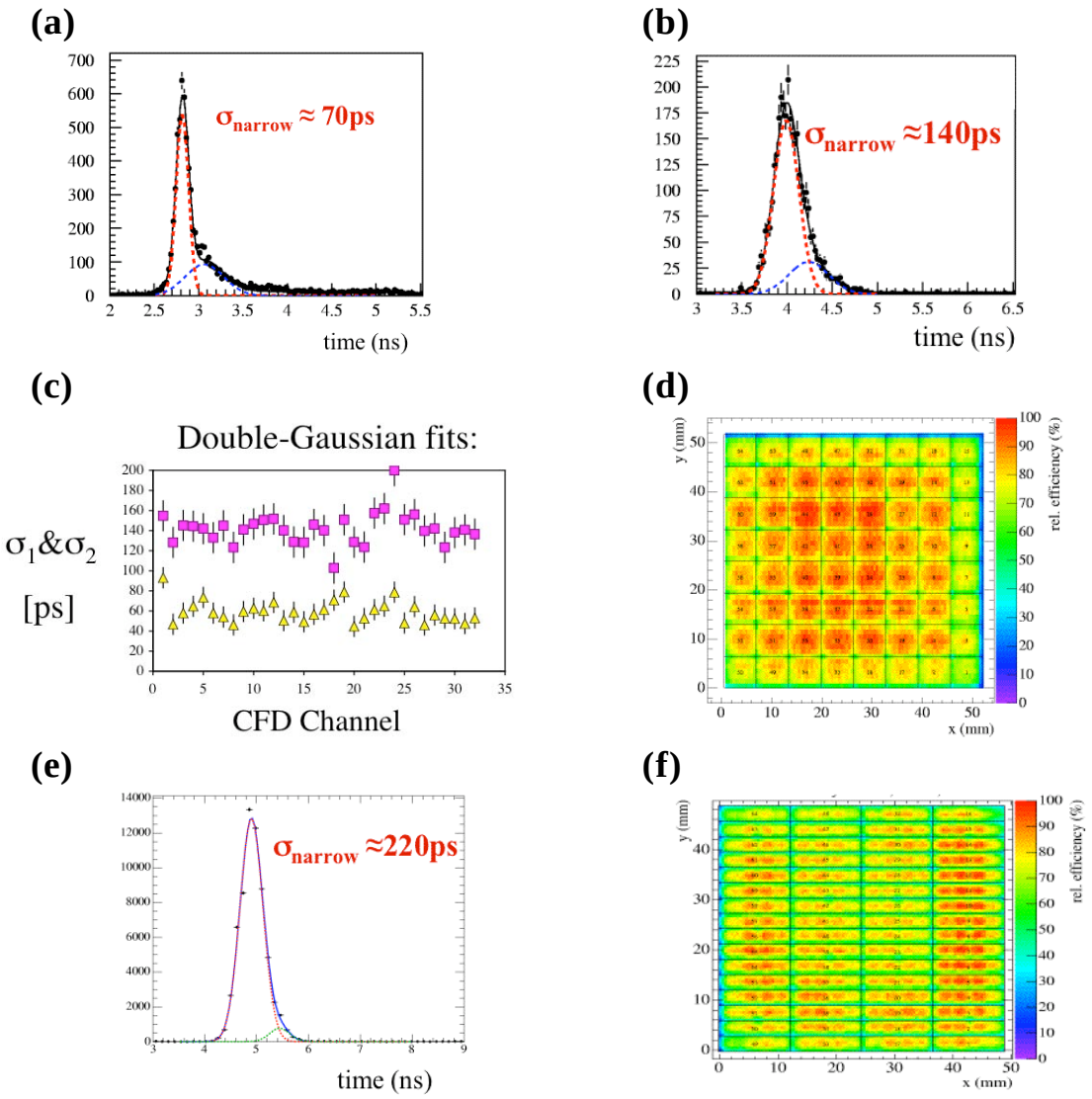

Fig. 6. Point-response timing resolution obtained with the PiLas light pulser and (a) 64-pixel Hamamatsu MaPMT H-8500, (b) 64-pixel Burle MCP-PMT 85011-501, (c) 64-pixel Burle MCP-PMT 85011-501 resolution across the 32 channels of SLAC CFD; double Gaussian fits are characterized by narrow and wide Gaussian curves. These resolutions do not average over pad edges, which would worsen the resolution due to the charge sharing. (d) A 2-D relative response of the Burle MCP-PMT 85011-501, normalized to the highest efficiency in the tube. (e) Point-response timing resolution of the 256-pixel Hamamatsu MaPMT H-9500, organized to rectangular pads of 3mm x 12mm in size. (f) A 2-D relative response of the Hamamatsu MaPMT H-9500, normalized to the highest efficiency in the tube. We used the Pilas laser diode wavelength of 407nm for pictures (d,e,f), and of 635nm for (a,b,c).

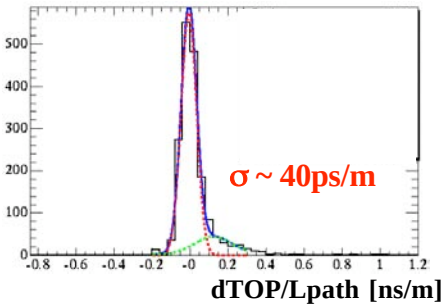

Fig. 7. A distribution of dTOP/Lpath for a single pad and indirect photons from position 1. This indicates that the chromatic broadening is about σ ~40ps/m.

studies. One way to improve the overall performance is to make sure that the region of the ring in the central region is measured well, for example, by better pixelization. The specifications of the photon detectors used presently in the Focusing DIRC prototype are shown in Tables 2 & 3.

Figure 6 shows examples of the point-response timing resolution, and a relative 2D-response normalized normalized to the highest efficiency in the tube. The point-response resolution was measured with light beam of less than 1 mm diameter aiming at the center of the pad, and attenuated to get a single photoelectron response. Therefore this result does not include the resolution degradation near pad's edges. For example, the Hamamatsu H-9500 MaPMT has worse resolution (Fig. 6e), which is likely due to the cross-talk and charge sharing. We use H-9500 MaPMT to improve the Cherenkov angle resolution by creating our own pixels, which provide finer sampling in y-direction and coarse in the x-direction - see Figures 2 and 6f. In addition, we expect a time dispersion in the prototype as a function of photon path length due to the chromatic effect, which grows at σ ~40 ps/meter, according to our test results – see Fig. 7.

TEST BEAM SETUP

We used a 10 GeV/c secondary electron beam produced on a Be target, and brought to the SLAC ESA test beam facility. The beam flux was less than 0.1-0.2 particles per pulse with a repetition rate of 10Hz typically. The beam spot size is a few mm in size and the beam divergence is less than ~0.2mrad. The beam spot was monitored in front of the bar with a fiber hodoscope made of 2x2mm^2 scintillation square fibers, which were readout by two 4x4 Hamamatsu R5900-L16 MaPMTs coupled to LeCroy ADC 2249A. In the next run, we plan to have a second hodoscope, which will be located behind the bar to reject possible slight contamination from showers in the bar. The system START time, which was used to start all TDCs in the system, was derived from the Linac RF pulse, which is the best possible method; however, because the cable bringing this pulse to ESA hall is very long, we had two local start counters available for possible corrections of the thermal effects (this was found not to be necessary in the analysis so far). The local start counters were either a fused silica double radiator (each 1.7cm thick, and rotated by ~47^o relative to the beam direction), or a 10cm thick BC-408 scintillator, both coupled to the Burle four-pad MCP-PMT, each pad coupled to the leading edge discriminator Phillips 706 with a 10mV threshold, Phillips TDC 7186 and LeCroy ADC 2249 to correct time for the pulse height variation. The timing resolution of the local start time was about σ ~35ps when averaged over all participating pads and two start counters. We used the lead glass block read out by the LeCroy ADC 2249 to reject a slight π^- contamination or the multiple electrons in the beam. The "good event" required a single electron hit in the lead glass and the fiber hodoscope.

The prototype was placed on a traversing table allowing easy movement of the bar to seven positions along its 3.6 m length. The total weight of the prototype was ~600 lb, the total weight of the support structure was ~1500 lb, i.e., a non-trivial mechanical challenge. The bar was aligned with a help of a laser to be perpendicular to the beam within less than ~1 mrad for all positions along the bar. The position of the bar along its length relative to the beam, and its repeatability, was known to ~1 mm.

EXPERIMENTAL RESULTS

The radiator refraction index is a function of wavelength. This leads to dispersion in the Cherenkov angle, the red photons corresponding to smaller angles compared to blue photons. While the red photons have an small path handicap from the production point to the detector, their group velocity is larger ($v_{group}(\lambda) = c_0 / n_{group} = c_0 / [n_{phase} - \lambda * dn_{phase}/d\lambda]$), so they arrive at the detector before the blue photons, resulting in an easily measured time dispersion of up to a few ns over the full range of Lpath. The final time

difference can be well measured already after photon path lengths of a few meters, and therefore the color dispersion at the Cherenkov angle production point can be corrected by time once the path lengths is sufficiently long. The Focusing DIRC prototype is the first RICH detector ever achieving this capability, thanks to its excellent time resolution of the photon detectors. There are various ways to parameterize the chromatic effect. We choose a parameterization as a function of TOP/Lpath variable because of its direct relationship to a quantity which is actually measured: time. Fig.8a shows a possible way to represent the chromatic behavior of the Focusing DIRC prototype in terms of a correlation between a change in the Cherenkov angle as a function of a change in TOP/Lpath = $1/v_{group}(\lambda)$, where the change is taken relative to their respective values evaluated at the most probable wavelength of 410 nm determined by the Focusing DIRC prototype efficiency; in other words, if a photon has an average wavelength of 410 nm, there is no chromatic correction. The shape of the curve in Fig. 8a is driven by the refraction index dependence on the wavelength and is evaluated for $\beta = 1$, which is the case for our test beam. There is a family of similar curves for different β. Fig. 8b shows a probability distribution as a function of dTOP/Lpath variable, indicating a FWHM range of ~140 ps/m. From here we see that the expected FWHM range of the Cherenkov angle correction is about ~10 mrads (Fig. 8a). Fig. 8c shows the same correlation in our data for a bar position 1 and using the indirect photons, which in this particular case travel over a long average distance of Lpath ~12 m. The line in Fig. 8c represents a fit in the profile plot. Fig. 8d shows a similar distribution using our full Geant 4 MC simulation. If we assume an ideal detector response without pixelization effects in the Geant 4 simulation, we get a curve on Fig. 8e.

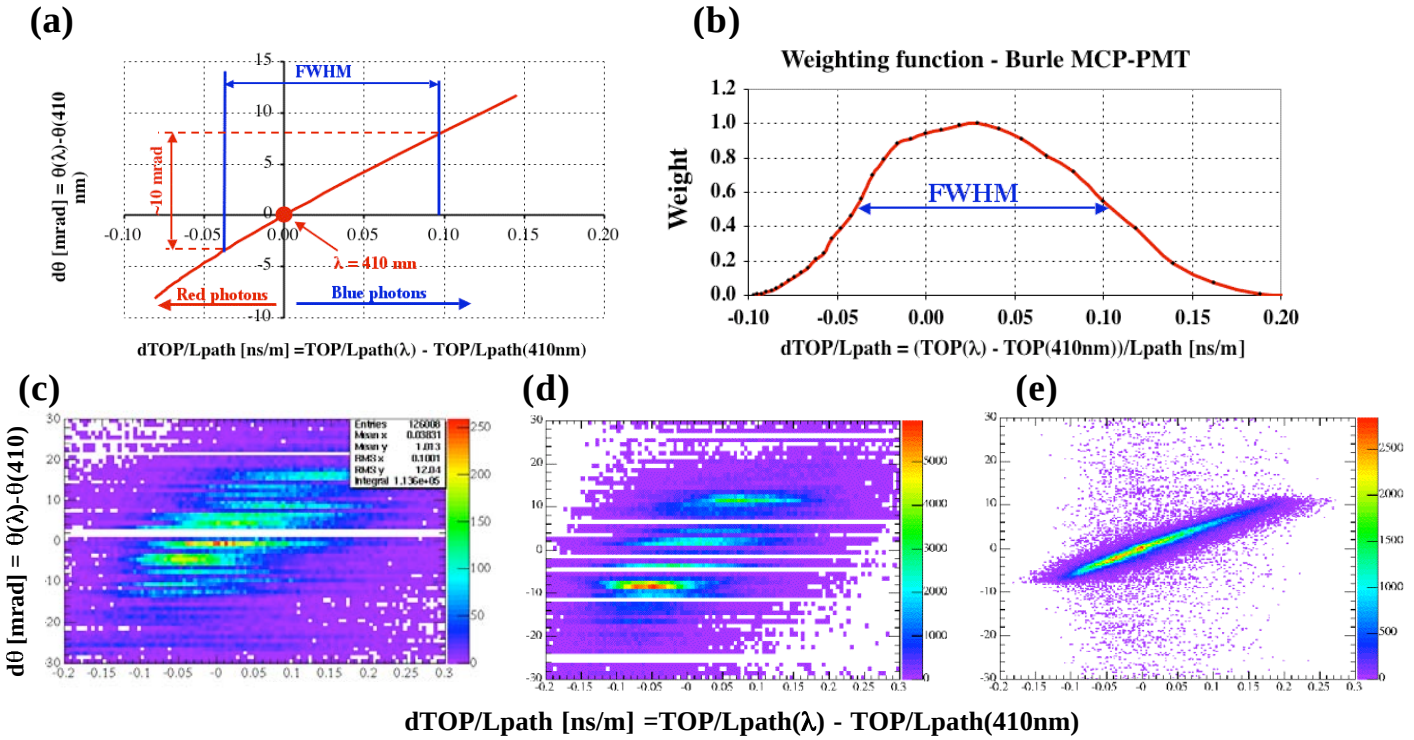

Fig. 8. (a) A correlation between a change in the Cherenkov angle as a function of a change in TOP/Lpath, where the change is taken relative to their respective values evaluated at the most probable wavelength of 410 nm determined by the Focusing DIRC prototype efficiency. (b) Weighting function for the Burle MCP-PMT, determined from the Cherenkov photon production yield and efficiencies, as a function a variable dTOP/Lpath. (c) The same correlation as in (a) shown for the data from the prototype. (d) The Geant 4 MC simulation assuming a detector pixelization and (e) an ideal case for a detector with infinitely good pixel and time resolution.

We are still evaluating the most effective method of implementing the chromatic correction in practice. The choices are as follows: (a) An analytical chromatic correction based on, for example, a spreadsheet calculation using existing theory – see Fig. 8a; this choice ignores the pixelization issues. (b) The Geant 4 Monte Carlo method with a pixelization – see Fig. 8d; this is a preferred method, at least in principle, but it does assume that the MC program simulates the real detector properly. (c) An empirical method relying on the data – see Fig. 8c; this method, however, assumes that all corrections to the data, such as the TDC calibration, or the MC program dependent constants, such as the Cherenkov angle assignments to each pixel, are correct. (d) A toy MC program, which has an advantage of greater simplicity compared to the Geant 4 MC. These are hard choices, as each technique has some pro and cons, but, at present we are leaning to use the chromatic correction based on the Geant 4 MC program simulation with a pixelization. For a real PID in a real detector, we will have to use a likelihood-based method to handle the corrections properly.

Figure 9 shows the measured pixel-based Cherenkov angle resolution from all pixels in the prototype, where data are not corrected for the chromatic error. Both data and the MC simulation points are shown with a preliminary systematic error of ~1 mrad.

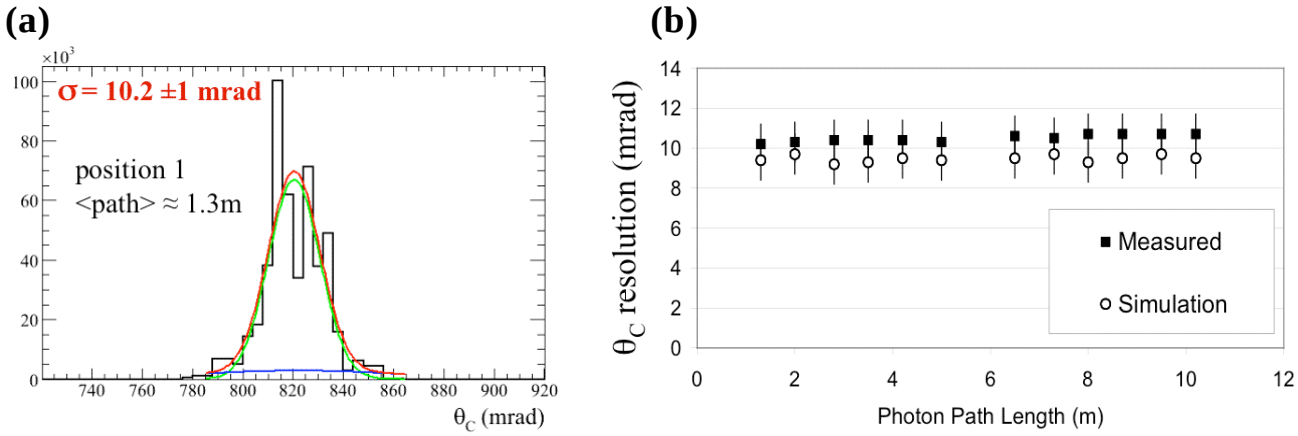

Fig. 9. Measured Cherenkov angle resolution using pixels without the chromatic correction for (a) position 1 and for the direct photons, and (b) the same as a function of the photon path in the bar length (Lpath), including the MC simulation.

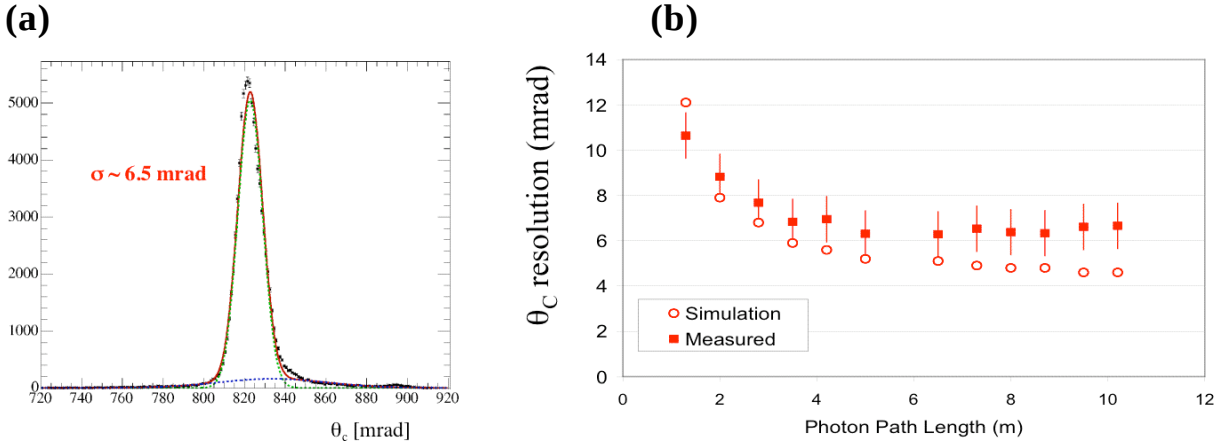

Fig. 10. Measured Cherenkov angle resolution using time without the chromatic correction for (a) position 1 and for the direct photons, and (b) the same as a function of the photon path in the bar length (Lpath), including the MC simulation.

Figure 10 shows the measured time-based Cherenkov angle resolution from all pixels in the prototype, where data are not corrected for the chromatic error. We use the measured TOP for each pixel and combine it with the associated path length (Lpath) to get group velocity v_g = Lpath/TOP, then we get the group

refraction index $n_g=c_0/v_g$, from there we get the phase refraction index $n=n(n_g)$, and finally the Cherenkov angle $\theta_c=\cos^{-1}(1/\beta n(\lambda))$, assuming $\beta=1$ for 10GeV/c electron beam. Comparing Figs. 9 & 10, one can see that the resolution based on time (TOP) is very good (6-7 mrads for Lpath>3-4 meters). This measurement is useful for checking the effect of timing resolution on θ_C, however, it cannot be used for the PID purposes because it assumes the particle ID ($\beta=1$). Again, both data and the MC simulation points are shown with a preliminary systematic error of ~1mrad.

It is useful to analyze the pixel data from slot 3 only, as this is the detector with pixel sizes (3 x 12 mm^2) we actually prefer for a final application because it samples the Cherenkov angle more finely and thus reduces the pixelization error contribution. Figure 11 shows the measured pixel-based Cherenkov angle resolution only from pixels of slot 3. We obtain clearly much better resolution compared to the pixel-based data combining all other slots: σ ~7 mrads almost independent of Lpath. The data are not corrected for the chromatic error. Both data and the MC simulation points show a preliminary systematic error of ~1 mrad.

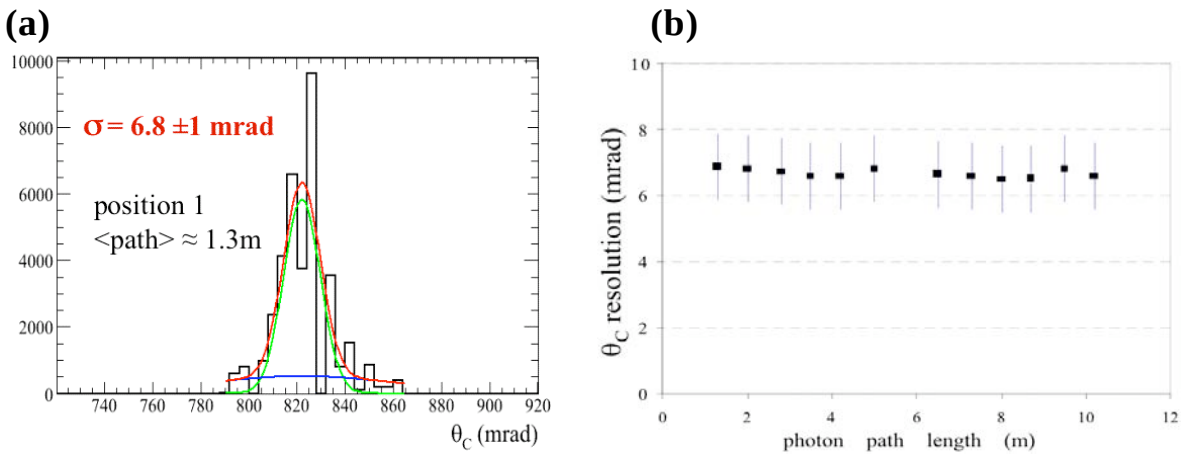

Fig. 11. Measured Cherenkov angle resolution using pixels from Slot 3 only, without the chromatic correction for (a) position 1 and for the direct photons, and (b) the same as a function of the photon path in the bar length (Lpath).

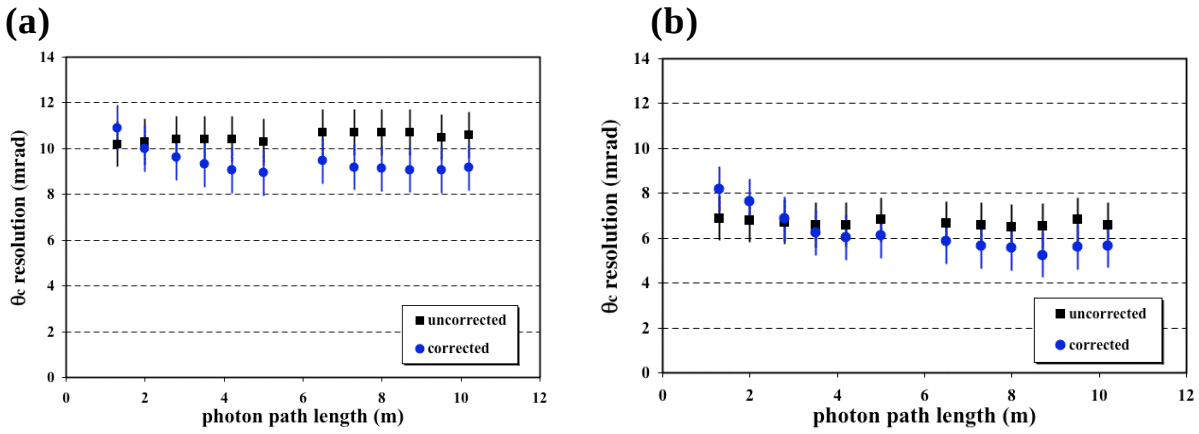

Fig. 12. Measured Cherenkov angle resolution using pixels with and without the chromatic correction as a function of photon path (Lpath) from (a) all slots, (b) slot 3 only.

Figure 12 shows the result of the chromatic correction to pixel-based data using time. Fig. 12a shows the chromatic correction for all slots. One can see that the time-based chromatic correction seems to improve the resolution by ~2 mrads and starts working for Lpath ≥2 meters. For shorter path lengths we would need

better time resolution. The observed improvement of ~1-2 mrads in the total Cherenkov angular error of over 10 mrad is more than we expect based our estimate of the chromatic error contribution alone, which is 3-4 mrad, so the magnitude of this effect is not yet understood. Fig. 12b shows the data with the chromatic correction for slot 3 only. The amount of correction is about 1 mrad for the longest path lengths and it starts working for Lpath ≥3 meters. This result is more consistent with our expectations. Again, for the correction to work at shorter path lengths we would need better timing resolution.

CONCLUSION

We have demonstrated that the Focusing DIRC prototype is an excellent tool to develop various possible concepts for the future fast Focusing RICH. We have demonstrated that the chromatic error contribution to the Cherenkov angle resolution can be corrected by fast timing, the first demonstration of this concept in a RICH detector. We believe that a 3D readout (θ,ϕ,t) makes the system more robust and helps to suppress the backgrounds. For the case of ~6x6 mm pixels, our θ_C resolutions measured in the beam test are quite competitive with BaBar-DIRC (σ ~9-10 mrad), however, in the case of ~12x3 mm pixels the θ_C resolution is considerably better (σ ~6-7 mrad). There are many remaining questions before the Focusing DIRC concept would be practical RICH detector in a real experiment, for example, issues such as: (a) development of appropriate detectors and associated electronics capable of operation in a high magnetic field of 15 kG, (b) questions how to handle a very large number of pixels in a final detector, (c) calibration, (d) aging, etc. We are slowly tackling these issues; for example: we plan (a) to install three new detectors with multi-alkali photocathodes, which will extend the wavelength response to the red region, thus, reducing the chromatic error contribution to the Cherenkov angle further, (b) to install a rectangular pads in additional detectors to provide finer sampling of the Cherenkov angle and reduce the pixelization effects, (c) to improve the TDC calibration scheme, and (d) to install ADCs on each pad to provide better photon position measurement.

ACKNOWLEDGEMENT

We would like to thank M. McCulloch and R. Reif for helping to construct the prototype, A. Scholz and T. Thurston for engineering help, J. Coleman and B.J. Wogsland for help running test beam shifts. We thank G. Gratta for providing us with the KamLand experiment's mineral oil.

REFERENCES

[1] I. Adam et al., "The DIRC Particle Identification System for the BaBar experiment," Nucl. Instr.&Meth., A538(2005)281-357.

[2] C. Field, T. Hadig, M. Jain, D.W.G.S. Leith, G. Mazaheri, B. Ratcliff, J. Schwiening, and J. Va'vra, "Novel photon detectors for Focusing DIRC prototype," Nucl. Instr. & Meth., A518(2004)565-568.

[3] C. Field, T. Hadig, D.W.G.S. Leith, G. Mazaheri, B. Ratcliff, J. Schwiening, J. Uher and J. Va'vra, "Development of photon detectors for the Focusing DIRC," Nucl. Instr. & Meth., A553(2005)96-106.

[4] J. Va'vra, J. Benitez, D.W.G.S. Leith, G. Mazaheri, B. Ratcliff, J. Schwiening, "A 30ps timing resolution for single photons with multi-pixel Burle MCP-PMT," submitted to Nucl. Instr. & Meth.